Thermal Imaging(Group 6)

Student: Changfan Chen

Mentors: Emad Boctor, Younsu Kim

1. Abstract

HIFU (High Intensity Focused Ultrasound), a non-invasive therapy is used to induce desired thermal dose to target tissue. It can ablate tissue with high energy instead of physical operation which can leave pain and permanent scar to patients. Due to minimal side effect on patients, it can be performed on complicate situations. MRI (Magnetic Resonance Imaging) temperature images are often used to monitor the ablation process. However, MRI is costly and some patients have restrictions. Ultrasound is a cost-effective medical imaging modality and requires less restrictions on operating environment. In this project, we propose a method to monitor the temperature using ultrasound channel data. Experiment is designed to collect channel data during HIFU ablation. Data is collected with the help of Younsu Kim, Chloe Audigier, Emran Mohammad Abu Anas and Ari Partanen. Thank them for help. The system alternates ablation phases and monitoring phases. In monitoring phase, ultrasound elements in the probe receive ultrasound wave sent from 256 HIFU elements sequentially. We use a ConvLSTM (Convolutional Long Short Term Memory) neural network to generate temperature images from collected channel data. The images are compared with the ones collected from MRI thermometry. Mean and max difference of each image are calculated to evaluate the performance of designed neural network. We achieve $0.57\pm0.33℃$ in mean error and $1.99\pm1.07℃$ in max error in axial image. In coronal image, we achieve $0.33\pm0.19℃$in mean error and $1.54\pm1.04℃$ in max error. The result shows the feasibility to use channel data and deep learning network to reconstruct the temperature image. To generalize the algorithm to more conditions and decrease the time to predict the temperature images. We proposed a pattern injection method. By subtracting the channel data after ablation by the ones before ablation, we acquire the pattern itself. With deep learning methods, the pattern can be used to predict the temperature images with vendor independence and high efficiency. The error in high temperature range is worse than in low temperature ones. However, the temperature difference is within $5℃$ which is acceptable.

2. Introduction

Traditional treatment to excise malignant tissue often leaves pain and permanent scar to patients. Also, it takes a long time for patients to recover from the surgery. In order to reduce the pain and damage of patients after surgery, many non-invasive technologies are developed. HIFU system is one of the most

widely used one[1], especially in treatments of prostate[2] and uterine fibroids[3]. Each element transmits continuous wave, and the acoustic energy is focused at target region. Consequently, the temperature in the target region is increased while minimally increasing temperature at surrounding tissues.

Although HIFU only focuses ultrasound pressure on target tissue, patients' motion can lead to inaccurate treatment. Thus, temperature monitoring is essential to guide the ablation process. MRI (Magnetic Resonance Imaging) thermometry is developed based on temperature sensitivity of proton resonance frequency[4]. This provides a real time imaging with high accuracy, but its high cost and strict requirement of nonmetal environment motivates people to develop monitoring methods using other medical imaging modalities[5]. For example, R. Seip and E.S. Ebbini developed a method to monitor temperature by measuring acoustic information based on discrete scattering model[6].

In order to extract both spatial features and temporal features, we use a ConvLSTM network to predict the temperature image. Through this approach, more possible properties can be learned to generate the temperature image. Instead of obtaining TOF from data, properties learned from ultrasound channel data may improve ultrasound thermometry without losing useful information.

To generalize the algorithm and decrease the time to monitor the temperature, we proposed pattern injection method. This method can predict the image within 3ms which is much quicker than previous ones. Simulation is conducted to generate pattern in channel which is used for network training.

3. LSTM Introduction

LSTM is a network developed from RNN which solves gradient vanishing and gradient explosion in training process. Compared with RNN, LSTM performs better in long sequence.

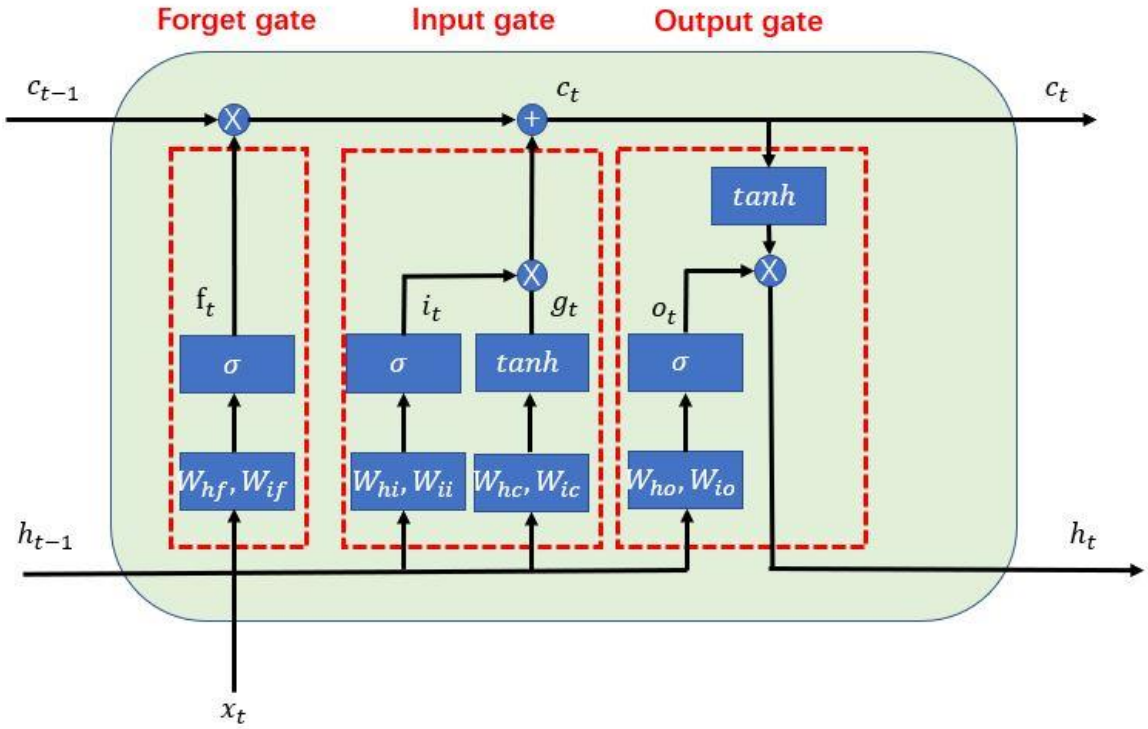

Fig. 1. LSTM cell

There are three gates in LSTM network which are forget gate, input gate and output gate. x_t represents the current input to the cell. c_t represents the output of the cell while c_{t-1} representing the output of previous cell and one of the input of the cell. h_t represents the state output of current cell while h_{t-1} is the state of previous cell. In forget gate, parameters are trained to determine how much previous output is remembered. In the input gate, the input of both x_t and h_{t-1} are used to determine how much input is remained, updated and added to c_{t-1}. The output gate determines the state to output by multiplying processed input by output of the cell. The equations are like below.

$$f_t = \sigma\left(W_{if}x_t + W_{hf}h_{t-1} + b_f\right)$$

$$g_t = \tanh\left(W_{hc}h_{t-1} + W_{ic}x_t + b_g\right)$$

$$i_t = \sigma(W_{hi}h_{t-1} + W_{ii}x_t + b_i)$$

$$o_t = \sigma(W_{ho}h_{t-1} + W_{io}x_t + b_o)$$

$$c_t = i_t \cdot g_t + c_{t-1} \cdot f_t$$

$$h_t = o_t \cdot tanhc_t$$

In ConvLSTM, the operation between parameters and arguments are changed from product to convolution which helps to extract spatial information and use it to do temporal prediction. Thus, both spatial and temporal features are considered. In our case, we use ConvLSTM because we need to extract spatial information like TOF and temporal information like TOF shift. Thus, ConvLSTM network matches our goal well.

4. Methods--HIFU Channel Data

4.1 Experiment and Data Collection

The system is illustrated in Figure 1 which is composed of an MRI compatible ultrasound probe with 128 elements, MRI machine to collect temperature image as ground truth, and HIFU system with 256 elements and a phantom. Phantom is made of 2% agar and 2% silicon-dioxide to mimic human tissue. The surface of HIFU system is covered by degassed water for acoustic coupling. The phantom is placed on the HIFU bed. Ultrasound probe is fixed with a holder on the top of the phantom to collect ultrasound signals. The whole setup is fixed in MRI gantry to obtain MRI temperature image and ultrasound channel data simultaneously.

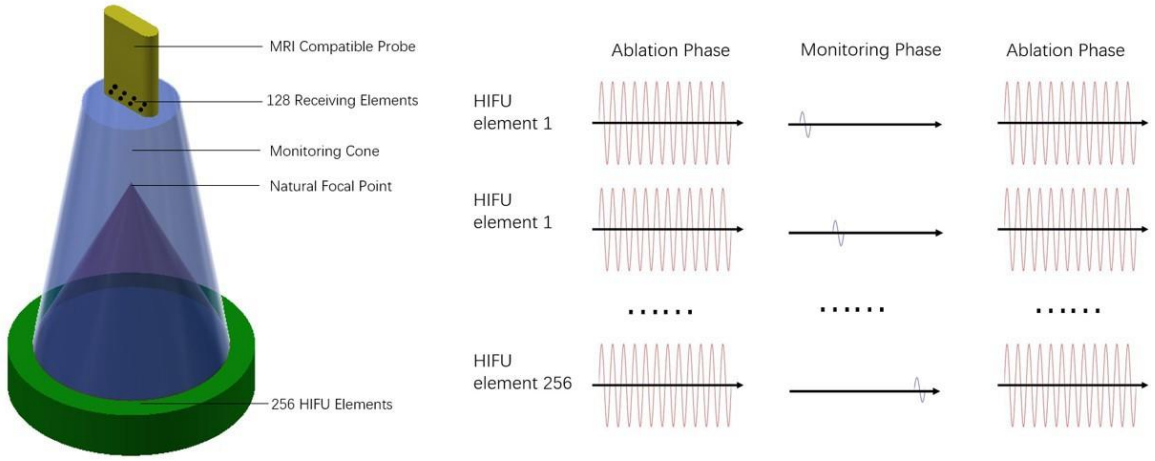

Fig. 2. HIFU experiment setup and timing diagram

Ultrasound waves transmit through target region and received by the probe. The ultrasound sampling frequency is 62.5 MHz. There are two phases : ablation phase and monitoring phase. First, in the ablation phase, HIFU elements transmit CW (continuous wave) with 78 Watts power for 5 seconds. The acoustic wave focuses on a target region to increase the temperature. Second, in monitoring phases, ultrasound pulses are transmitted with 2 Watts power sequentially. The pinging interval of each HIFU element is 3 ms. When the last element finishes pinging, the system finishes monitoring phase. Our system alternates ablation phase and monitoring phase for six cycles. Since the low power pinging signal is transmitted sequentially, the temperature change during monitoring phase is negligible. The monitoring time is less than 0.8 second so that we assume the temperature in monitoring phase does not change. Temperature images are generated by MRI thermometry every 1.5 seconds. By averaging the MRI temperature images right before the beginning of monitoring phase and right after the last pinging, we obtain the temperature image of the monitoring phase generated by MRI. Before experiment, the initial phantom temperature is 20 Celsius degrees. The temperature after the final ablation is 45 Celsius degrees.

By comparing signal received by a certain element, we are able to acquire the TOF shift. In Figure 3, all the figures share the same HIFU element and receiving element. Considering TOF, there are both signal shift in Figure 3(b) and Figure 3(d). This shows TOF changes with temperature. The TOF shift in Figure 3(b) is 960 ns while TOF shift in Figure 3(d) is 2270 ns. The higher temperature difference results in the larger the TOF shift. In addition, we can observe from Figure 3(a) and Figure 3(c) that the signal amplitude in second monitoring phase is smallest while the one in forth phase is biggest. In the experiment temperature range, the signal attenuates more as the temperature increases. Thus, in second monitoring phase where temperature is low, the signal attenuates most when being received.

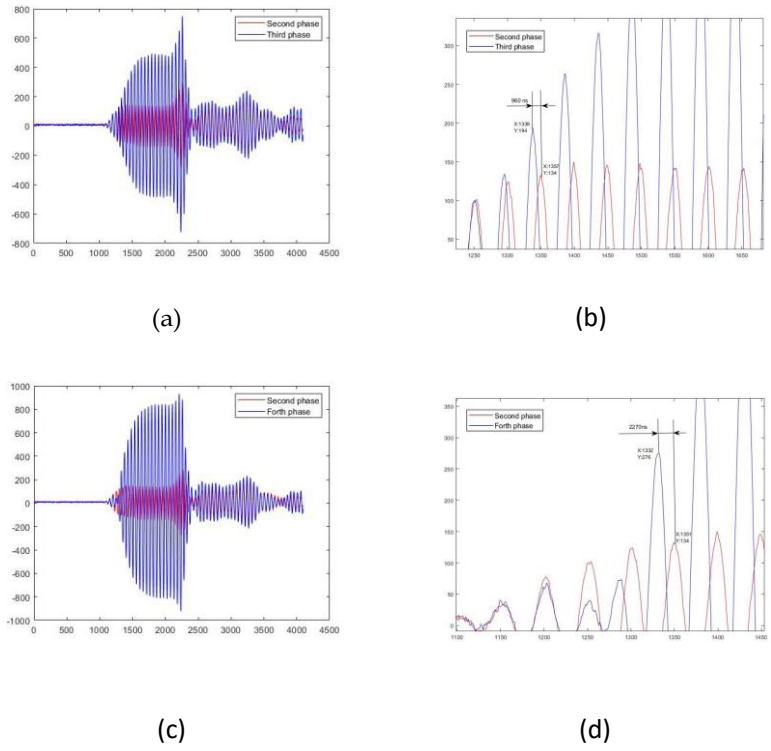

(a) (b)

(c) (d)

Fig. 3. Example of received signal at different monitoring phases

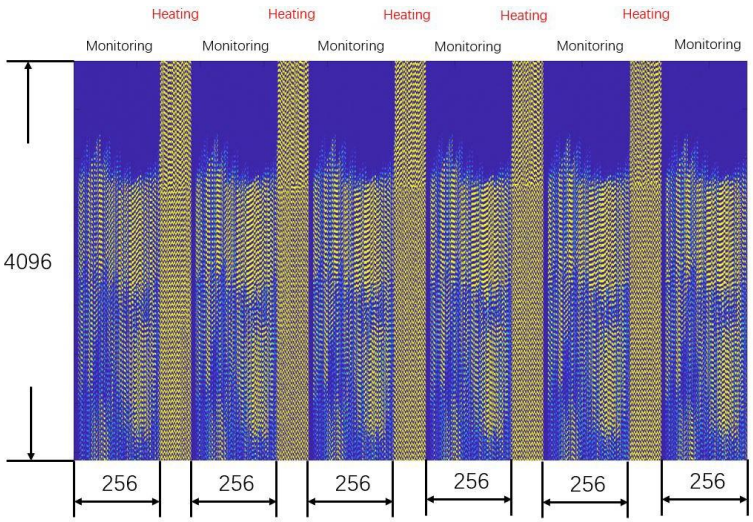

Fig. 4. Channel data received by one probe element

4.2 Network Design

We repeated and collected data from three experiments. We picked 128 elements randomly from 256 HIFU elements to make one data set. For a certain probe element in an experiment, we sampled 128 HIFU elements randomly for 20 times. Since we had three experiments and 128 probe elements, we sampled HIFU elements $128 \times 3 \times 20$ times which is 7680 times. Then we generated val- idation and test set similarly for 3 times at each of element and dataset. In this case, correlation between training set and test set is low since 128 combination of 256 elements is very large number.

The size of data we collected in each monitoring phase is $4096 \times 256 \times 128$ since the sample number is 4096 with 256 HIFU elements and 128 ultrasound probe elements. There are 256 elements in the HIFU system transmitting pulses sequentially and 128 elements in the probe receiving the signal. For a single receiving element, the input is the concatenation signal of initial monitoring phase and current monitoring phase. The pulse arrives at first 2048 samples, thus we only use first 2048 samples to reduce the input size to reduce number of parameters in the network. Therefore, the size of input is $2 \times 2048 \times 128$.

TOF shift and attenuation coefficient shift is essential to derive the temperature[8]. These properties can be learned from convolution operation in the network while the difference is learned by ConvLSTM with historical input. Convolution operation is done with the output of ConvLSTM. Also, location vectors are added in the network as another input. It is composed of relative coordinates of HIFU elements with respect to a certain ultrasound element in the probe. The concatenated layer is connected with few fully connected layers. After that, the layer is reshaped into a 40 by 40 array. It passes through convolution

and transposed convolution layers and be flattened. Finally, it is connected to a fully connected layer with 400 size vector output and be reshaped to be a 20 by 20 image. The output of the network is the temperature image, and the MRI temperature images serve as ground truth.

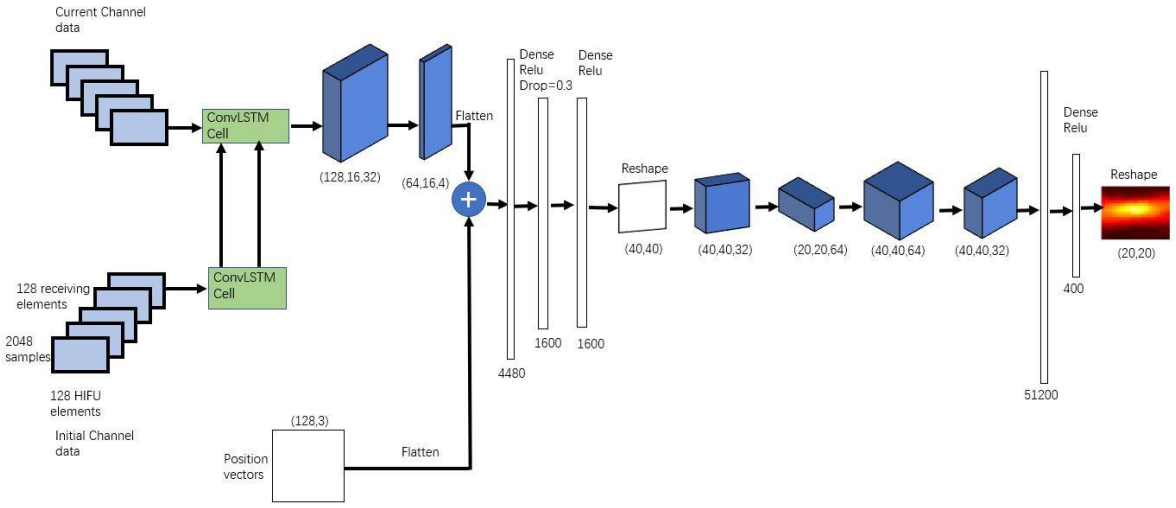

Fig. 5. Deep learning network

Network is trained with early stopper to avoid over-fitting. If the validation error does improve within 10 epochs, the network will stop training. The learning rate of the network is 0.0015. Since accuracy on the temperature in the center is more important than background, ROI (Region of interest) is selected to be a 20×20 area at the center of the natural focus. For each image, we calculate the mean absolute error and maximum absolute error of all pixels on the image. On the test set, the mean error of axial image is $0.57 \pm 0.33℃$while the maximum error is $1.99 \pm 1.07℃$. The maximum difference is $9.16℃$. The mean error of coronal image is $0.33 \pm 0.19℃$ while the maximum error is $1.54 \pm 1.04℃$. The maximum difference is $9.04℃$. The error of coronal image is smaller than that of axial image due to smaller intersection of heated area.

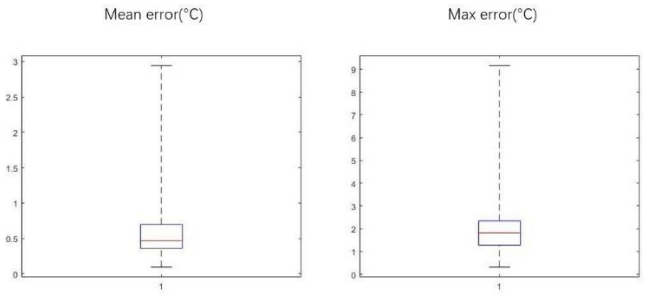

(a) Axial

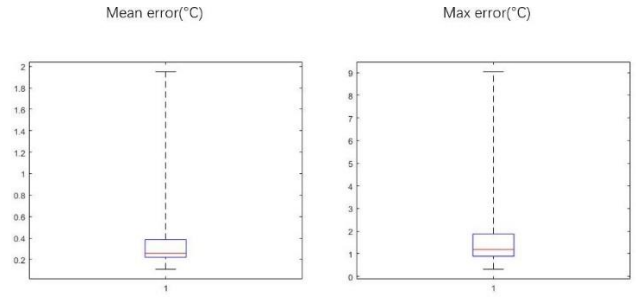

(b) Coronal

Fig. 6. Box plot of mean error and max error

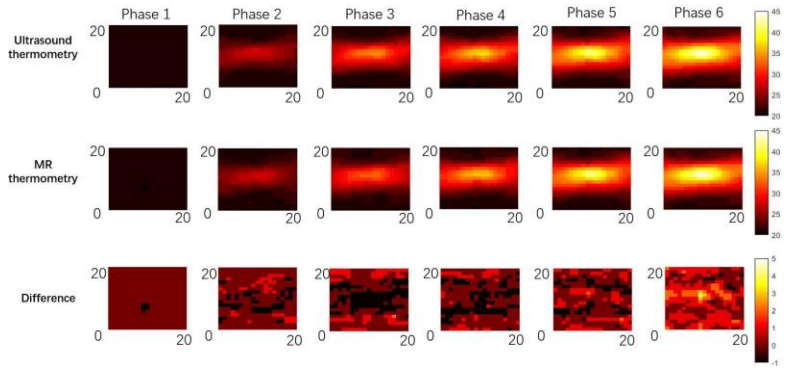

(a) Axial images

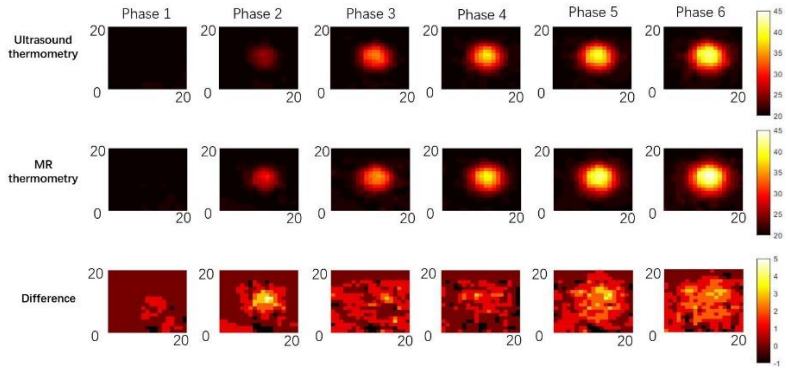

(b) Coronal Images

Fig. 7. The MRI image, reconstructed image and their difference of one receiving element at 6 different monitoring phase. Phase 1 is the one before the first ablation

5. Methods--Pattern Injection

Although the method above is promising and accurate enough, the time used to monitor the temperature is 3ms x 256 which is too long for real time guidance. Also, it needs too many HIFU elements which are not always available in all devices. Thus, we proposed a pattern injection method where only one element is placed under the heat source and transmitting pulses. By receiving these pulses from probe, we acquire channel data. However, the data is relevant to background which means once the background changes, the channel data will change. In fact, we want our method to be robust to any background.

Actually, by subtracting current channel data by the channel data at initial status, we remove the background and leave only pattern. I did simulation on this to acquire channel data.

5.1 Temperature Simulation

The simulation is done on matlab K-wave simulation tool. It is useful and convenient to do ultrasound simulation. Four structures are defined: kgrid, medium, source and sensor. In order to speed the simulation, we defined a 2D space which is kgrid. The space is 80mm by 38 mm with 128x128 grids. The medium is defined as water. We define the source to be a single element under heat source with random position which generalizes the data. The sensor is defined to be along the first row of the work space. By using kspaceFirstOrder2D, it takes me 2days to generate 120 data sets. We use 80 of them to train and 40 of them to test.

In order to conduct simulation in different temperature, we first conduct thermal simulation. Similarly, by defining kgrid, medium and heat source, we use kWaveDiffusion to generate temperature images.

Actually, speed of sound changes with temperature so we transfer the temperature images into speed of sound map which is defined in the medium previous simulation. Thus, we can do simulation in different temperatures. In fact, we define 660 seconds where first 600s the temperature increases with RF ablation and in the rest 60s the workspace cools down. The temperature starts from 37 degree Celsius.

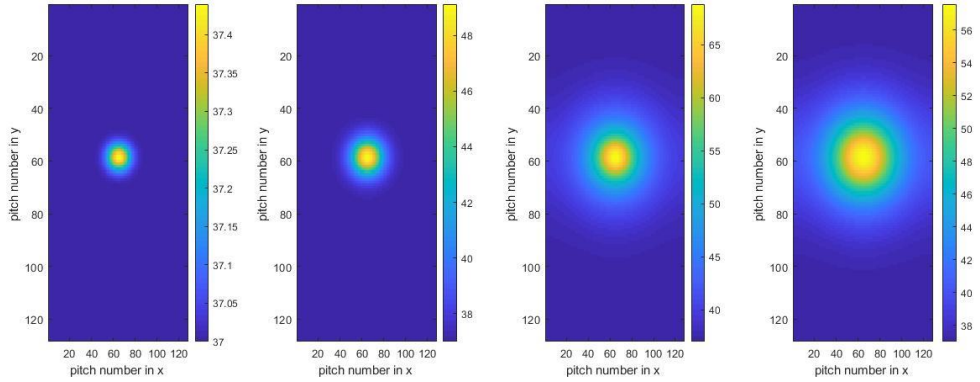

Fig. 8. Temperature images

5.2 Channel data simulation

With these temperature images, we are able to collect channel data. By temperature to SOS function provided by Chloe, I changed the medium of different timestep to mimic the condition that temperature changes. In order to generalize the pattern, I set random variable for the pulse. The pulse has random cycles ranging from two to six. Each pule has random gap between them ranging from 5 to 15 samples. There are 2 to 4 pulses. The pulses look like follows.

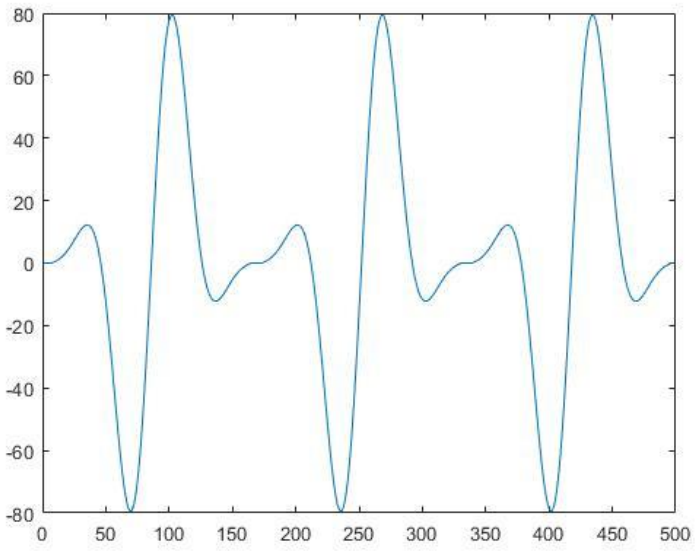

Fig. 9. Pulse transmitted from source element

Also, the position of source elements is randomized. Since it is below the heat source which is around the center, we set the x coordinate of source to be in range [60,78]mm, y coordinate of source to be in range [7,31]mm. Then we are able to collect channel data of pattern in randomized way. In order to decrease the size of input to network, we do the cross correlation in element wise. That is to say, every second, the signal

received by element does cross correlation operation with initial signal. Then we pick 64 samples in the center to train the network. That help us to maintain as much information as we want while decreasing the data capacity.

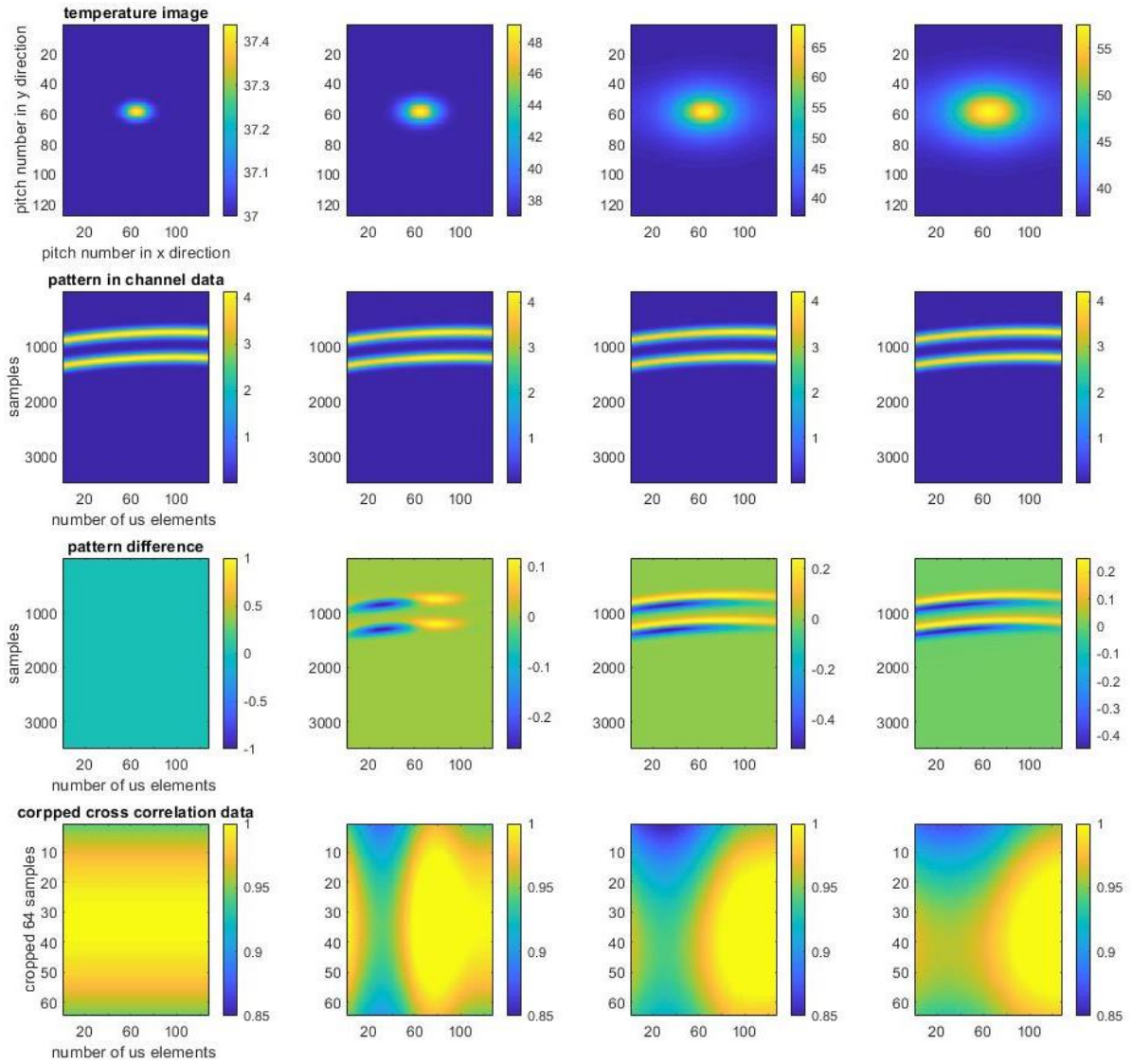

Fig. 10. Pulse transmitted from source element. First row are temperature images. Second row are patterns in channel data. Third row is pattern difference with first pattern. Forth row is the elementwise cross correlation data

Problem in simulation

If change channel data into db, we can see that there are some artifacts. By looking into the location of artifacts we found that the sensors receive the signal once the source transmit it without any delay. After discussion, we thought it may be the problem of kwave simulation tool. However, the artifact becomes much smaller in 2D case which can be ignored. Thus, we conduct simulation in 2D case.

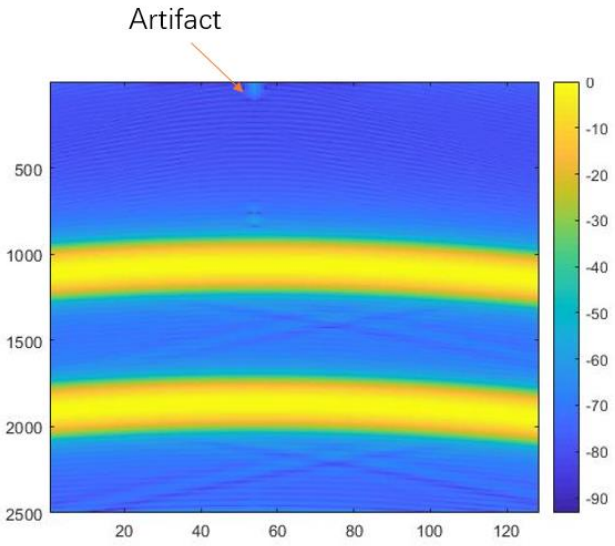

Fig. 11. Artifact in channel data

5.3 Analysis of cross correlation data

In the beginning, all signals are cross correlated with initial signal which is itself. Thus, the plot has high temperature in the middle regardless of which element it is. Then, as temperature increases, the element in the middle receives the signals with high temperature, which means there is time of flight shift which decrease the cross correlation value. As temperature keep increasing, the area where intensities are small becomes larger because area with high temperature has been enlarged. Finally, as the temperature cools down, it starts to diffusion. Thus, the cross correlation value in the middle tends to be even. However, on two edges, since the signal received does not change with same temperature, so they are always the same as ones in the first image.

5.4 Result

Emran helps me to design the network and I train the network to validate this method. The result shows the good performance in low temperature but bad ones on high temperature. It makes sense because in low temperature the speed of sound changes with temperature linearly and in high temperature it changes with speed of sound nonlinearly.

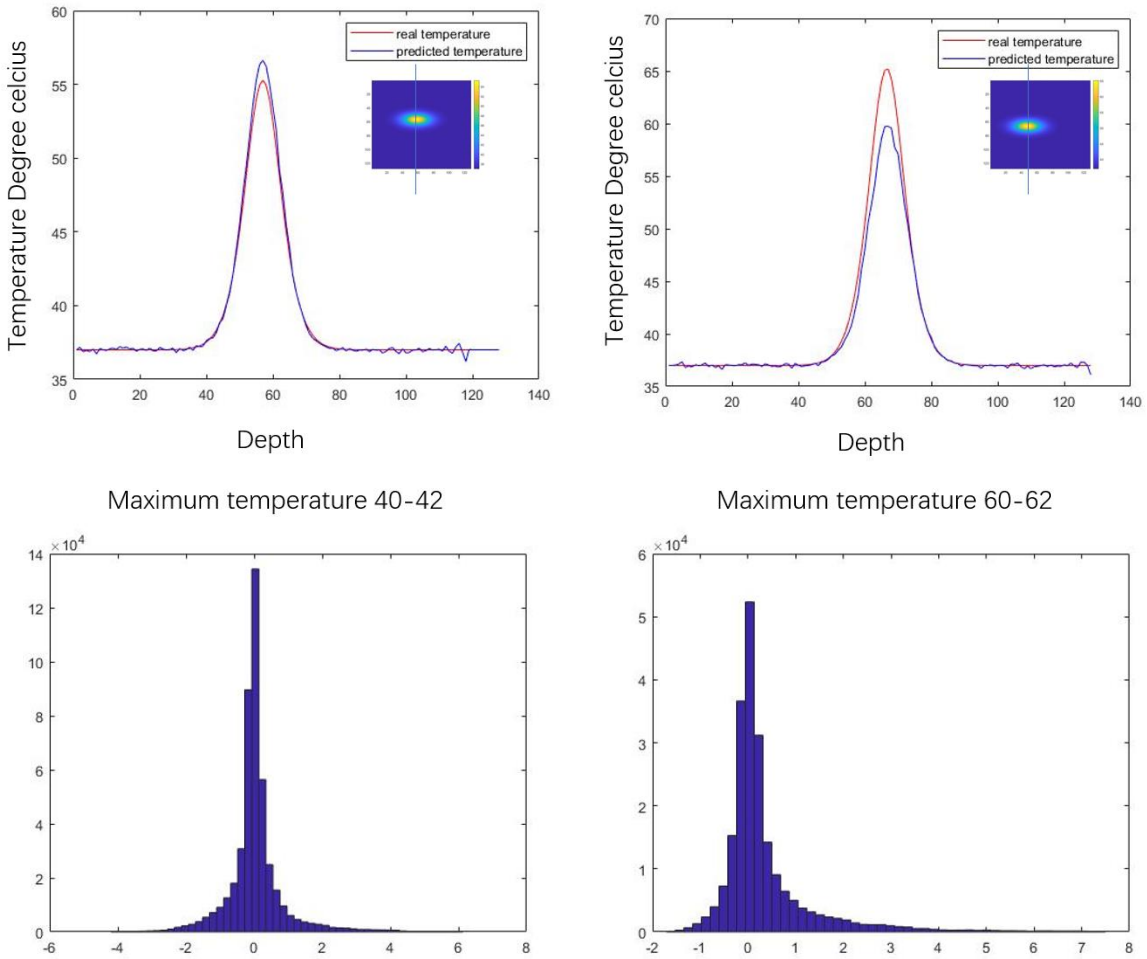

Fig. 12. First row shows the temperature images with different max temperature. Second row shows the error of all data set where maximum temperature is in different range

6. Conclusion

The method to collect channel data from HIFU signals does not need extra devices and is very convenient. However, it takes long time and needs to conduct many experiments to collect data. In order to improve this, we proposed a pattern injection method which is based on simulation data and more efficient. Also, it can be vendor independent. The method shows promising result on predicting temperature images. However, if the temperature is high, it is still hard to predict. Also, since channel data is not always available in all ultrasound devices, it is better to have pattern in B mode images. Thus, in the future, we plan to simulate pattern on bmode images and train the network.

7. Management Summary

7.1 Meeting and management

I meet once or twice a week with Younsu Kim, who is a very kind PHD student in MUSIIC lab. Every week, we have a group meeting with Professor Emad Boctor who provides any needed help and inspires me about lots of great ideas. Also, group meeting helps me to get familiar with others project and inspires mine. Once I meet with any problem, I would contact Younsu Kim and Dr Emad Boctor to solve them. Their feedback help me to better understand the project and avoid lots of problems. All codes are shared on JH box and Thin6 in case of any problem. My laptop crashed once, but thanks to Professor Taylor's advice, I still had backup on Thin6.

7.2 Planned vs Accomplished

This semester, I contributed to collecting data with the help of Younsu Kim, Chloe Audigier and Ari Partanen. Thank them for their help. Then I do the data processing and designed multiple networks to predict temperature images. However, the hospital and NIH is not available during this period, I am not able to do more experiments. Thus, under the advice of Professor Emad Boctor, I look into another problem to propose another method and do simulation on it. Below is the initial deliverable and updated ones. Since I can not do experiments, I can not finish initial expected and maximum deliverables. I update the deliverable once I change the direction. I finish the minimum deliverable and expected deliverable. I did deep learning, data processing and simulation. As for the deep learning of pattern deduction approach, I did not design the network good enough to predict temperature images. However, Emran Mohammad Abu Anas helped me to design. I help him to train the network and get the result. Thus, I do not include this work into my maximum deliverable.

	Original	Updated
Minimum	Video of comparison between prediction and ground truth in experiment	code written in Python which generate temperature image from channel data
	code written in Python which generate temperature image from channel data	Save code of data processing and documentation & report
	Save code of data processing and documentation & report	IUS Abstract
Expected	Report of process and test 7 experiments dataset from the HIFU experiment	Report on simulation
	Written report of difference between performance of TOF and channel data	Code and documentation on simulation
Maximum	Written report on vivo experiments	Report on pattern deduction approach
		Code and documentation on deep learning

7.3 Next steps

Since channel data is not always available to all ultrasound platform, if we can train the network with pattern in bmode images, we can better popularize this technology. Thus, next step would be conducting

simulation of pattern on bmode images. Currently, I meet the problem that it takes too long to do bmode simulation. I would keep working on it to do bmode simulation.

7.4 Lessons Learned

I finished design the network early and got good result. However, I always find that I process the data by mistake or the data is imperfect. Thus, I need to repeat the process and redesign the network. Thus, the most important thing I learn is that data is always the most important in deep learning. Without right data, the result does not make any sense even it is good. Also, I found some impractical aspect in my project. For example, channel data is not always available in all ultrasound devices. In the future, before working on project, I need to have deeper understanding of ultrasound technologies and their practical use.d

8. Acknowledgement

Thank Professor Emad Boctor for advising me on this project and inspiring me a lot of great ideas. I acquire lots of knowledge every time I talk with him. Also, thank Younsu Kim who has almost twice meetings a week with me to answer my problems and discuss with me. He is very patient to my questions and kind to offer any help. Also, thank Hyunwoo Song for helping me to learn ultrasound knowledge. Thank Professor Taylor's advices on management and presentations. He always points out my problems and helps me to improve.

9. References

1. Kennedy J E, Ter Haar G R, Cranston D. High intensity focused ultrasound: surgery of the future[J]. The British journal of radiology, 2003, 76(909): 590-599.

2. Murat F J L, Gelet A. Current status of high-intensity focused ultrasound for prostate cancer: technology, clinical outcomes, and future[J]. Current urology re- ports, 2008, 9(2): 113.

3. Chapman A, Ter Haar G. Thermal ablation of uterine fibroids using MR-guided focused ultrasound-a truly non-invasive treatment modality[J]. European radiology, 2007, 17(10): 2505-2511.

4. Graham S J, Stanisz G J, Kecojevic A, et al. Analysis of changes in MR properties of tissues after heat treatment[J]. Magnetic Resonance in Medicine: An Official Journal of the International Society for Magnetic Resonance in Medicine, 1999, 42(6): 1061- 1071.

5. Maass-Moreno R, Damianou C A, Sanghvi N T. Noninvasive temperature estimation in tissue via ultrasound echo-shifts. Part II. In vitro study[J]. The Journal of the Acoustical Society of America, 1996, 100(4): 2522-2530.

6. Seip R, Ebbini E S. Noninvasive estimation of tissue temperature response to heating fields using diagnostic ultrasound[J]. IEEE Transactions on Biomedical Engineering, 1995, 42(8): 828-839.

7. Kim Y, Audigier C, Ellens N, et al. A novel 3D ultrasound thermometry method for HIFU ablation using an ultrasound element[C]//2017 IEEE international ultrasonics symposium (IUS). IEEE, 2017: 1-4.

8. Audigier C, Kim Y, Boctor E. A Novel Ultrasound Imaging Method for 2D Temper- ature Monitoring of Thermal Ablation[M]//Imaging for Patient-Customized Simu- lations and Systems for Point-of-Care Ultrasound. Springer, Cham, 2017: 154-162.

9. Kim Y, Audigier C, Ellens N, et al. Low-Cost Ultrasound Thermometry for HIFU Therapy Using CNN[C]//2018 IEEE International Ultrasonics Symposium (IUS). IEEE, 2018: 1-9.